Queueing-Based Analysis of Broadcast Optical Networks *

Martin W. McKinnon[†], George N. Rouskas[‡], Harry G. Perros[‡]

[†]Georgia Tech Research Institute, Atlanta, GA 30332

[‡]Department of Computer Science, North Carolina State University, Raleigh, NC 27695-7534

bill.mckinnon@gtri.gatech.edu, {rouskas,hp}@csc.ncsu.edu

Abstract

We consider broadcast WDM networks operating with schedules that mask the transceiver tuning latency. We develop and analyze a queueing model of the network in order to obtain the queue-length distribution and the packet loss probability at the transmitting and receiving side of the nodes. The analysis is carried out assuming finite buffer sizes, non-uniform destination probabilities and two-state MMBP traffic sources; the latter naturally capture the notion of burstiness and correlation, two important characteristics of traffic in high-speed networks. We present results which establish that the performance of the network is a complex function of a number of system parameters, including the load balancing and scheduling algorithms, the number of available channels, and the buffer capacity. We also show that the behavior of the network in terms of packet loss probability as these parameters are varied cannot be predicted without an accurate analysis. Our work makes it possible to study the interactions among the system parameters, and to predict, explain and fine tune the performance of the network.
Keywords: Optical networks, Markov modulated Bernoulli process (MMBP), wavelength division multiplexing (WDM), discrete-time queueing networks

1 Introduction

It has long been recognized that Wavelength Division Multiplexing (WDM) will be instrumental in bridging the gap between the speed of electronics and the virtually unlimited bandwidth available within the optical medium. The wavelength domain adds a significant new degree of freedom to network design, allowing new network concepts to be developed. For a local area environment with a small number of users, the WDM broadcast-and-select architecture has emerged as a simple and cost-effective solution. In such a LAN, nodes are connected through a passive broadcast star coupler and communicate using transceivers tunable across the network bandwidth.

A significant amount of research effort has been devoted to the study of WDM architectures in recent years [4]. The performance analysis of these architectures has been typically carried out assuming uniform traffic and memoryless arrival processes [16, 3, 5]. However, it has been established that, in order to study correctly the performance of a network, one needs to use models that capture the notion of burstiness and correlation in the traffic stream, and which permit non-uniformly distributed destination probabilities [8, 9]. Two studies of optical networks that use non-Poisson traffic models appeared recently in [13, 14]. The work in [13] derives a stability condition for the HiPeR-ℓ reservation protocol, while [14] studies the effects of wavelength conversion in wavelength routing networks. We are not aware of any queueing-based studies of broadcast WDM networks.

In this paper we revisit the well known broadcast-and-select WDM architecture in an attempt to investigate the performance of broadcast optical networks under more realistic traffic assumptions and finite buffer capacity. Specifically, we develop a queueing-based decomposition algorithm to study the performance of a network operating under schedules that mask the transceiver tuning latency [6, 12, 1, 2, 11]. The analysis is carried out using Markov Modulated Bernoulli Process (MMBP) arrival models that naturally capture the important characteristics of traffic in high-speed networks. Additionally, our analysis allows for unequal traffic flows to exist between sets of nodes. Our work makes it possible to study the complex interaction among the various system parameters such as the arrival processes, the number of available channels, and the scheduling and load balancing algorithms. To the best of our knowledge, such a comprehensive performance analysis of a broadcast WDM architecture has not been done before.

The next section presents the queueing and traffic model and provides some background information. The performance analysis of the network is presented in Sections 3 and 4, numerical results are given in Section 5, and we conclude the paper in Section 6.

2 System Model

In this section we introduce a model for the media access control (MAC) layer in a broadcast-and-select WDM LAN. The model consists of two parts, a queueing network and a transmission schedule. We also present a traffic model to characterize the arrival processes to the network.
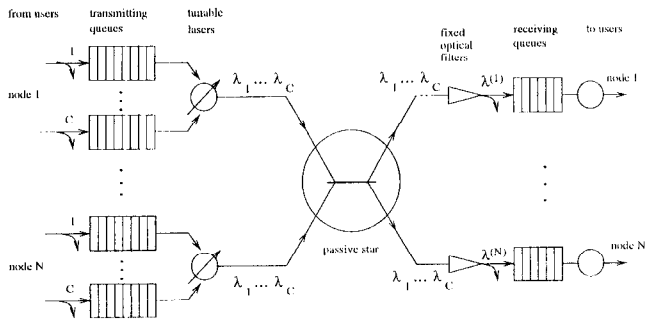
Figure 1: Queueing model of a broadcast WDM architecture with N nodes and C wavelengths

2.1 The Queueing Model

We consider an optical network architecture with N nodes communicating over a broadcast passive star that can support $C \leq N$ wavelengths, $\lambda_1, \cdots, \lambda_C$ (see Figure 1). Each node is equipped with a laser that enables it to inject signals into the optical medium, and a filter capable of receiving optical signals. The laser at each node is tunable over all available wavelengths. The optical filters, on the other hand, are fixed to a given wavelength. Let $\lambda(j)$ denote the receiving wavelength of node j. Since $C \leq N$, a set $\mathcal{R}_c$ of nodes may be sharing a single wavelength λ_c: $\mathcal{R}_c = \{j \mid \lambda(j) = \lambda_c\}$, $c = 1, \cdots, C$.

Each node consists of a transmitting side and a receiving side, as Figure 1 illustrates. New packets (from users) arrive at the transmitting side of a node i and are buffered at a finite capacity queue, if the queue is not full. Otherwise, they are dropped. As Figure 1 indicates, the buffer space at the transmitting side of each node is assumed to be partitioned into C independent queues. Each queue c, $c = 1, \ldots, C$, at the transmitting side of node i contains packets destined for the receivers which listen to wavelength λ_c. This arrangement eliminates the head-of-line problem, and permits a node to send several packets back-to-back when tuned to a certain wavelength. We let $B_{ic}^{(in)}$ denote the capacity of the transmitting queue at node i corresponding to channel λ_c.

Packets buffered at a transmitting queue are sent on a FIFO basis onto the optical medium by the node's laser. A schedule (discussed shortly) ensures that transmissions on a given channel will not collide, hence a transmitted packet will be correctly received by its destination node. Upon arriving at the receiving side of its destination node, a packet is placed in another finite capacity buffer before it is passed to the user for further processing. We let $B_j^{(out)}$ denote the buffer capacity of the receiving queue at node j. Packets arriving to find a full receiving queue are lost. Packets in a receiving queue are also served on a FIFO basis.

Packets in the network have a fixed size and the nodes operate in a slotted mode. Since there are N nodes but $C \leq N$ channels, the passive star (i.e., each of the C channels) must run at a rate $\frac{N}{C}$ times faster than the rate at which users at each node can generate or receive packets ($\frac{N}{C}$ need not be an integer). In other words, the MAC-to-network interface runs faster than the user-to-MAC interface. Thus, we distinguish between arrival slots (which correspond to the packet transmission time at the user rate) and service slots (which are equal to the packet transmission time at the channel rate within the network). Obviously, the duration of
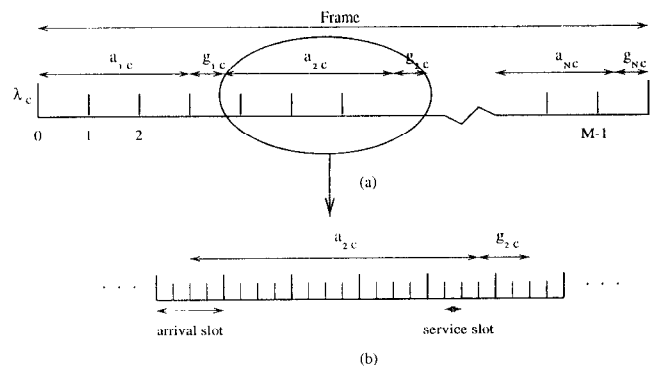
a service slot is equal to $\frac{C}{N}$ times that of an arrival slot. All N nodes are synchronized at service slot boundaries. Using timing information about service slots and the relationship between service and arrival slots one can derive the timing of arrival slots. Hence, we assume that all users are also synchronized at arrival slot boundaries.

2.2 Transmission Schedules

One of the potentially difficult issues that arises in a WDM environment, is that of coordinating the various transmitters/receivers. Some form of coordination is necessary because (a) a transmitter and a receiver must both be tuned to the same channel for the duration of a packet's transmission, and (b) a simultaneous transmission by one or more nodes on the same channel will result in a collision. The issue of coordination is further complicated by the fact that tunable transceivers need a non-negligible amount of time to switch between wavelengths.

Several scheduling algorithms have been proposed for the problem of scheduling packet transmissions in such an environment [6, 12, 1, 2, 11]. Although these algorithms differ in terms of their design and operation, surprisingly the resulting schedules are very similar. A model that captures the underlying structure of these schedules is shown in Figure 2. In such a schedule, node i is assigned a_{ic} contiguous service slots for transmitting packets on channel λ_c. These a_{ic} slots are followed by a gap of $g_{ic} \geq 0$ slots during which no node can transmit on λ_c. This gap may be necessary to ensure that the laser at node $i + 1$ has sufficient time to tune from wavelength λ_{c-1} to λ_c before it starts transmission. Note that in Figure 2 we have assumed that an arrival slot is an integer multiple of service slots. This may not be true in general, and it is not a necessary assumption for our model. Observe also that, although a schedule begins and ends on arrival slot boundaries, the beginning or end of transmissions by a node does not necessarily coincide with the beginning or end of an arrival slot (although they are, obviously, synchronized with service slots).

We assume that transmissions by the transmitting queues onto wavelength λ_c follow a schedule as shown in Figure 2. This schedule repeats over time. Each frame of the schedule consists of M arrival slots. Quantity a_{ic}, $i = 1, \cdots, N$, $c = 1, \cdots, C$, can be seen as the number of service slots per frame allocated to node i, so that the node can satisfy the required quality of service of its incoming traffic intended for wavelength λ_c. By fixing a_{ic}, we indirectly allocate a certain amount of the bandwidth of wavelength λ_c to node i.

Figure 2: (a) Schedule for channel λ_c, and (b) detail corresponding to node 2

This bandwidth could, for instance, be equal to the effective bandwidth [7] of the total traffic carried by node i on wavelength λ_c. In general, the estimation of the quantities a_{ic}, $i = 1, \cdots, N$, $c = 1, \cdots, C$, is part of the connection admission algorithm [7], and it is beyond the scope of this paper. We note that as the traffic varies, a_{ic} may vary as well. In this paper, we assume that quantities a_{ic} are fixed, since this variation will more likely take place over larger scales in time.

2.3 Traffic Model

The arrival process to each transmitting queue of the network is characterized by a two-state Markov Modulated Bernoulli Process (MMBP), hereafter referred to as 2-MMBP. A 2-MMBP is a Bernoulli process whose arrival rate varies according to a two-state Markov chain. It captures the notion of burstiness and the correlation of successive interarrival times, two important characteristics of traffic in high-speed networks. For details on the properties of the 2-MMBP, the reader is referred to [10]. (We note that the algorithm for analyzing the network was developed so that it can be readily extended to MMBPs with more than two states.)

We assume that the arrival process to transmitting queue c, $c = 1, \ldots, C$, of node i, $i = 1, \cdots, N$, is given by a 2-MMBP characterized by the transition probability matrix $\mathbf{Q}_{ic}$, and by $\mathbf{A}_{ic}$ as follows:

$$\mathbf{Q}_{ic} = \left[\begin{array}{cc} q_{ic}^{(00)} & q_{ic}^{(01)} \\ q_{ic}^{(10)} & q_{ic}^{(11)} \end{array} \right] \quad \text{and} \quad \mathbf{A}_{ic} = \left[\begin{array}{cc} \alpha_{ic}^{(0)} & 0 \\ 0 & \alpha_{ic}^{(1)} \end{array} \right] \quad (1)$$

In (1), $q_{ic}^{(kl)}, k, l = 0, 1$, is the probability that the 2-MMBP will make a transition to state l, given that it is currently at state k. Obviously, $q_{ic}^{(k0)} + q_{ic}^{(k1)} = 1$, $k = 0, 1$. Also, $\alpha_{ic}^{(0)}$ $(\alpha_{ic}^{(1)})$ is the probability that an arrival will occur in a slot at state 0 (1). Transitions between states of the 2-MMBP occur only at the boundaries of *arrival* slots. We assume that the arrival process to each transmitting queue is given by a different 2-MMBP. From (1) and [10], the steady-state arrival probability for the arrival process to this queue is

$$\gamma_{ic} = \frac{q_{ic}^{(10)}\alpha_{ic}^{(0)} + q_{ic}^{(01)}\alpha_{ic}^{(1)}}{q_{ic}^{(01)} + q_{ic}^{(10)}} \quad (2)$$

Let r_{ij} denote the probability that a packet generated at node i will have j as its destination node. We will refer to $\{r_{ij}\}$ as the *routing* probabilities; this description implies that the routing probabilities can be node-dependent and non-uniformly distributed. The destination probabilities of successive packets are not correlated. That is, in a node, the destination of one packet does not affect the destination of the packet behind it. Given these assumptions, the probability that a packet generated at node i will have to be transmitted on wavelength λ_c is:

$$r_{ic} = \sum_{j \in \mathcal{R}_c} r_{ij}, \quad i = 1, \cdots, N \quad (3)$$

Obviously, the relationship between r_{ic} and γ_{ic} is given by $r_{ic} = \gamma_{ic}/(\sum_{k=1}^{C} \gamma_{ik})$.

3 Queueing Analysis

In this section we analyze the queueing network shown in Figure 1, which represents the tunable-transmitter, fixed-receiver optical network under study. The arrival process to
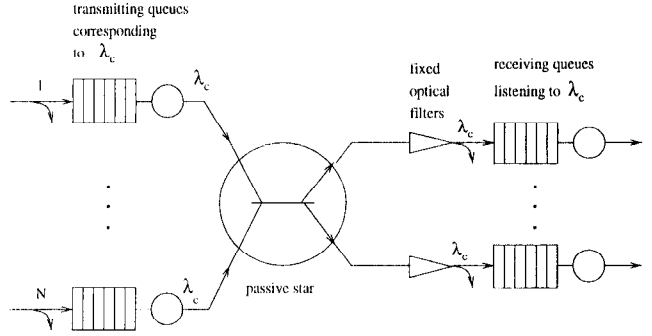

Figure 3: Queueing sub-network for wavelength λ_c

each transmitting queue is assumed to be a 2-MMBP, and the access of the transmitting queues to the wavelengths is governed by a schedule similar to the one described in Section 2.2. We analyze this queueing network in order to obtain the queue-length distribution in a transmitting or receiving queue, from which performance measures such as the packet-loss probability can be obtained.

3.1 Transmitting Side Analysis

We first note that the original queueing network can be decomposed into C sub-networks, one per wavelength, as in Figure 3. For each wavelength λ_c, the corresponding sub-network consists of N transmitting queues, and all the receiving queues that listen to wavelength λ_c. Each transmitting queue i of the sub-network is the one associated with wavelength λ_c in the i-th node. These transmitting queues will transmit to the receiving queues of the sub-network over wavelength λ_c. Note that, due to the independence among the C queues at each node, the transmission schedule (i.e., the fact that different nodes transmit on the same wavelength at different times), and the fact that each receiver listens to a specific wavelength, this decomposition is exact. In view of this decomposition, it suffices to analyze a single sub-network, since the same analysis can be applied to all other sub-networks.

Consider now the sub-network for wavelength λ_c. We will analyze this sub-network by decomposing it into individual transmitting and receiving queues. As discussed in the previous section, each transmitting queue i of the sub-network is only served for a_{ic} consecutive service slots per frame. During that time, no other transmitting queue is served. Transmitting queue i is not served in the remaining slots of the frame. In view of this, there is no dependence among the transmitting queues of the sub-network, and consequently each one can be analyzed in isolation in order to obtain its queue-length distribution. (Each receiving queue will also be considered in isolation in Section 3.2.)

From the queueing point of view, the queueing network shown in Figure 3 can be seen as a polling system in discrete time. Despite the fact that polling systems have been extensively analyzed, we note that very little work has been done within the context of discrete time (see, for example, [18]). In addition, this particular problem differs from the typical polling system since we consider receiving queues, which are not typically analyzed in polling systems.
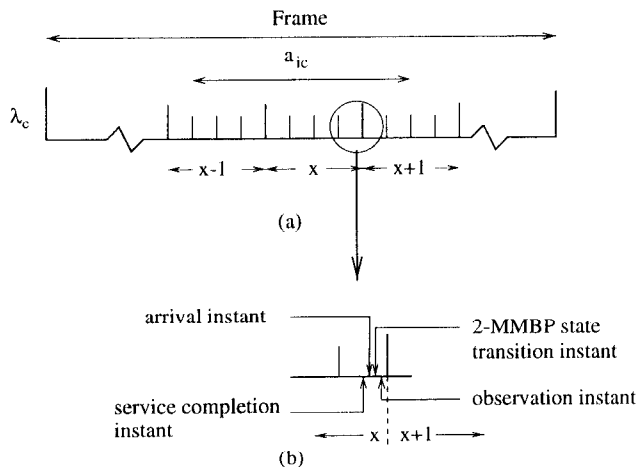
Figure 4: (a) Service period of transmitting queue i on channel λ_c, and (b) detail showing the relationship among service completion, arrival, 2-MMBP state transition, and observation instants within a service and an arrival slot

3.1.1 The Queue-Length Distribution of a Transmitting Queue

Consider transmitting queue i of the sub-network for λ_c in isolation. This queue receives exactly a_{ic} service slots on wavelength λ_c, as shown in Figure 4(a). The block of a_{ic} service slots may not be aligned with the boundaries of the arrival slots. For instance, in the example shown in Figure 4(a), the block of a_{ic} service slots begins at the second service slot of arrival slot $x - 1$, and it ends at the end of the second service slot in arrival slot $x + 1$. Here, $x - 1$, x, and $x + 1$ represent the arrival slot number within a frame.

For each arrival slot, define $v_{ic}(x)$ as the number of service slots allocated to transmitting queue i, that lie within arrival slot x [1]. Then, in the example in Figure 4(a), we have: $v_{ic}(x-1) = 3, v_{ic}(x) = 4, v_{ic}(x+1) = 2$, and $v_{ic}(x') = 0$ for all other x'. Obviously, we have

$$\sum_{x=0}^{M-1} v_{ic}(x) = a_{ic} \qquad (4)$$

We analyze transmitting queue i by constructing its underlying Markov chain embedded at arrival slot boundaries. The order of events is as follows. The service (i.e., transmission) completion of a packet occurs at an instant just before the end of a service slot. An arrival may occur at an instant just before the end of an arrival slot, but after the service completion instant of a service slot whose end is aligned with the end of an arrival slot. The 2-MMBP describing the arrival process to the queue makes a state transition immediately after the arrival instant. Finally, the Markov chain is observed at the boundary of each arrival slot, *after* the state transition by the 2-MMBP. The order of these events is shown in Figure 4(b).

The state of the transmitting queue is described by the tuple (x, y, z), where:

- x represents the arrival slot number within a frame $(x = 0, 1, \cdots, M - 1)$,

- y indicates the number of packets in the transmitting queue $(y = 0, 1, \cdots, B_{ic}^{(in)})$, and

- z indicates the state of the 2-MMBP describing the arrival process to this queue, that is, $z = 0, 1$.

It is straightforward to verify that, as the state of the queue evolves in time, it defines a Markov chain. Let $\oplus$ denote modulo-M addition, where M is the number of arrival slots per frame. Then, the transition probabilities out of state (x, y, z) are given in Table 1. Note that, the next state after (x, y, z) always has an arrival slot number equal to $x \oplus 1$. In the first row of Table 1 we assume that the 2-MMBP makes a transition from state z to state z' (from (1), this event has a probability $q_{ic}^{(zz')}$ of occurring), and that no packet arrives to this queue during the current slot (from (1) and (3), this occurs with probability $1 - \alpha_{ic}^{(z)}$). Since at most $v_{ic}(x \oplus 1)$ packets are serviced during arrival slot $x \oplus 1$, and since no packet arrives, the queue length at the end of the slot is equal to $\max\{0, y - v_{ic}(x \oplus 1)\}$. In the second row of Table 1 we assume that the 2-MMBP makes a transition from state z to state z' and a packet arrives to the queue. This arriving packet cannot be serviced during this slot, and has to be added to the queue. Finally, the expression for the new queue length ensures that it will not exceed the capacity $B_{ic}^{(in)}$ of the transmitting queue.

The probability transition matrix of this Markov chain is straightforward to derive from Table 1. This matrix defines a *p-cyclic* Markov chain [15], and therefore it can be solved using any of the techniques for p-cyclic Markov chains in [15, ch. 7]. We have used the LU decomposition method in [15] to obtain the steady state probability $\pi_{ic}(x, y, z)$ that at the end of arrival slot x, the 2-MMBP is in state z and the transmitting queue has y packets. The steady-state probability that the queue has y packets at the end of slot x, independent of the state of the 2-MMBP is:

$$\pi_{ic}(x, y) = \sum_{z=0,1} \pi_{ic}(x, y, z) \qquad (5)$$

Finally, we note that all of the results obtained in this subsection can be readily extended to MMBP-type arrival processes with more than two states.

3.2 Receiving Side Analysis

Consider the sub-network for wavelength λ_c in Figure 3, and observe that the arrival process to the receiving queues sharing λ_c is the combination of the departure processes from the transmitting queues corresponding to λ_c. An interesting aspect of the departure process from the transmitting queues is that for each frame, during the sub-period a_{ic} we only have departures from the i-th queue. This period is then followed by a gap g_{ic} during which no departure occurs. This cycle repeats for the next transmitting queue. Thus, in order to characterize the overall departure process offered as the arrival process to these receiving queues, it suffices to characterize the departure process from each transmitting queue, and then combine them. (We note that this overall departure process is quite different from the typical superposition of a number of departure processes into a single stream, where, at each slot, more than one packet may be departing.) The overall departure process is completely defined given the queue-length distribution of all transmitting

---

[1] In Figure 4, we assume that each arrival slot contains an integral number of service slots. If this is not the case, $v_{ic}(x)$ is defined as the number of service slots that end within arrival slot x (i.e., if there is a service slot that lies partially within arrival slots x and $x + 1$, it will be counted in $v_{ic}(x + 1)$).

Table 1: Transition probabilities out of state (x,y,z) of the Markov chain

Current State	Next State	Transition Probability
(x,y,z)	$(x \oplus 1, \max\{0, y - v_{ic}(x \oplus 1)\}, z')$	$q_{ic}^{(zz')}(1 - \alpha_{ic}^{(z)})$
(x,y,z)	$(x \oplus 1, \min\{B_{ic}^{(in)}, \max\{0, y - v_{ic}(x \oplus 1)\} + 1\}, z')$	$q_{ic}^{(zz')}\alpha_{ic}^{(z)}$

queues in the sub-network (which may be obtained using the analysis in Section 3.1), since then the probability that a packet will be transmitted on channel λ_c in any given service slot is known.

However, the individual arrival processes to each of the receiving queues listening on λ_c are not independent. Specifically, if j and j' are two receivers on λ_c, and there is a transmission from transmitting queue i to receiving queue j in a given service slot, then there can be no arrival to receiving queue j' in the same service slot. We will nevertheless make the assumption that these arrival processes are indeed independent, and that each is an appropriately thinned (based on the routing probabilities) version of the departure process from the transmitting queues. Note that this is an approximation only when there are multiple nodes with receivers fixed on channel λ_c. This assumption allows us to decompose the sub-network of Figure 3 into individual receiving queues and to analyze each of them in isolation [2].

3.2.1 The Queue-Length Distribution of a Receiving Queue

As in the previous section, we obtain the queue-length distribution of receiving queue j at arrival slot boundaries. During an arrival slot x a packet may be transmitted to the user from the receiving queue. However, during slot x, there may be several arrivals to this receiving queue from the transmitting queues. Let (x, w) be the state associated with receiving queue j, where

- x indicates the arrival slot number within the frame ($x = 0, 1, \cdots, M - 1$), and

- w indicates the number of packets at the receiving queue ($w = 0, 1, \cdots, B_j^{(out)}$).

We assume the following order of events. A packet will begin to depart from the receiving queue at an instant immediately after the beginning of an arrival slot and the departure will be completed just before the end of the slot. A packet from a transmitting queue arrives at an instant just before the end of a service slot, but before the end-of-departure instant of an arrival slot whose end is aligned with the end of the service slot. Finally, the state of the queue is observed just before the end of an arrival slot and after the arrival associated with the last service slot has occurred (see Figure 5(b)).

[2] We also note that the approach of analyzing each receiving queue in isolation gives correct results for the individual receiving queues; after all, in steady-state, the probability that a packet transmitted by node i on λ_c will have j as its destination will equal the routing probability r_{ij}. This approach is an approximation only when one attempts to combine results from individual receiving queues to obtain the overall performance for the network. It is possible to apply techniques to adjust for this approximation when aggregating individual results [17]. We will not consider such techniques here, instead we will only concentrate on individual queues.
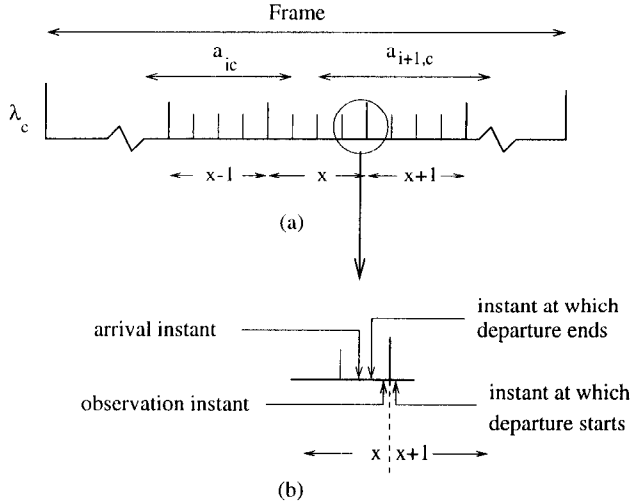

Figure 5: (a) Arrivals to receiving queue j from transmitting queues i and $i + 1$, and (b) detail showing the relationship of departure, arrival, and observation instants

Let $u_j(x)$ be the number of service slots of any transmitting queue on channel λ_c within arrival slot x. We have:

$$u_j(x) = \sum_{i=1}^{N} v_{ic}(x) \tag{6}$$

where $v_{ic}(x)$ is as defined in (4). Quantity $u_j(x)$ represents the maximum number of packets that may arrive to receiving queue j within slot x. In the example of Figure 5(a) where we show the arrival slots during which packets from transmitting queues i and $i + 1$ may arrive to receiving queue j, we have: $u_j(x - 1) = v_{ic}(x - 1) = 4$, $u_j(x) = v_{ic}(x) + v_{i+1,c}(x) = 1 + 2 = 3$, and $u_j(x + 1) = v_{i+1,c}(x + 1) = 4$.

Observe now that (a) at each state transition x advances by one (modulo-M), (b) exactly one packet departs from the queue as long as the queue is not empty, (c) a number $s \leq u_j(x \oplus 1)$ of packets may be transmitted from the transmitting queues to receiving queue j within arrival slot $x \oplus 1$, and that (d) the queue capacity is $B_j^{(out)}$. Then, the transition probabilities out of state (x, w) for this Markov chain can be obtained from Table 2.

In Table 2, $L_i(s_i \mid x)$ is the probability that transmitting queue i transmits s_i packets to receiving queue j given that the system is at the end of arrival slot x (in other words, it is the probability that s_i packets are transmitted within slot $x \oplus 1$) [3]. To obtain $L_i(s_i \mid x)$, define r'_{ij} as the conditional

[3] Since in most cases only one or two transmitting queues will transmit to the same channel within an arrival slot (refer also to Figure 2), the summation and product in the expression in the last column of Table 2 do not necessarily run over all N values of i, only over one

Table 2: Transition probabilities out of state (x, w) of the Markov chain

Current State	Next State	Transition Probability
$(x, 0)$	$(x \oplus 1, \min\{B_j^{(out)}, s\}), 0 \le s \le u_j(x \oplus 1)$	$\sum_{s_1 + \cdots + s_N = s} \prod_{i=1}^{N} L_i(s_i \mid x)$
$(x, w), w > 0$	$(x \oplus 1, \min\{B_j^{(out)}, w + s\} - 1), 0 \le s \le u_j(x \oplus 1)$	$\sum_{s_1 + \cdots + s_N = s} \prod_{i=1}^{N} L_i(s_i \mid x)$

probability that a packet is destined for node j, given that the packet is destined to be transmitted on λ_c, the receive wavelength of node j:

$$r'_{ij} = \frac{r_{ij}}{\sum_{k \in \mathcal{R}_c} r_{ik}} = \frac{r_{ij}}{r_{ic}} \quad (7)$$

Define $\pi_{ic}(y \mid x)$ as the conditional probability of having y packets at the i-th transmitting queue given that the system is observed at the end of slot x:

$$\pi_{ic}(y \mid x) = \frac{\pi_{ic}(x, y)}{\pi_{ic}(x)} = M \, \pi_{ic}(x, y) \quad (8)$$

Then, for $r'_{ij} < 1$, the probability $L_i(s_i \mid x)$ is given by

$$L_i(s_i \mid x) = \begin{cases} 0, s_i > v_{ic}(x \oplus 1) \\ \sum_{y=s_i}^{B_{ic}^{(in)}} \pi_{ic}(y \mid x) \begin{pmatrix} \min\{y, v_{ic}(x \oplus 1)\} \\ s_i \end{pmatrix} (r'_{ij})^{s_i} \\ (1 - r'_{ij})^{\min\{y, v_{ic}(x \oplus 1)\} - s_i}, s_i \le v_{ic}(x \oplus 1) \end{cases} \quad (9)$$

Expression (9) can be explained by noting that transmitting queue i will transmit s_i packets to receiving queue j during arrival slot $x \oplus 1$ if (a) $v_{ic}(x \oplus 1) \ge s_i$, (b) node i has $y \ge s_i$ packets in its transmitting queue for λ_c at the beginning of the slot (equivalently, at the end of slot x), and (c) exactly s_i of $\min\{y, v_{ic}(x \oplus 1)\}$ packets that will be transmitted by this queue in this arrival slot are for receiver j. Expression (9) represents the "thinning" of the arrival processes to the various receiving queues of the sub-network using the r'_{ij} routing probabilities, and discounts the correlation among arrival streams to the different queues. Expression (9) is the crux of our approximation for the receiving side of the network.

If $r'_{ij} = 1$, in which case j is the only node listening on wavelength λ_c, the expression for $L_i(s_i \mid x)$ must be modified as follows (recall that there is no approximation in this case):

$$L_i(s_i \mid x) = \begin{cases} 0, & s_i > v_{ic}(x \oplus 1) \\ \pi_{ic}(s_i \mid x), & s_i < v_{ic}(x \oplus 1) \\ \sum_{y=s_i}^{B_{ic}^{(in)}} \pi_{ic}(y \mid x), & s_i = v_{ic}(x \oplus 1) \end{cases} \quad (10)$$

Expressions (9) and (10) are based on the assumption that $v_{ic}(x \oplus 1) < B_{ic}^{(in)}$ which we believe is a reasonable one. In the general case, quantity $v_{ic}(x \oplus 1)$ in both expressions must be replaced by $\min\{v_{ic}(x \oplus 1), B_{ic}^{(in)}\}$.

The transition matrix of the Markov chain defined by the evolution of the state (x, w) of receiving queue j also defines a p-cyclic Markov chain. We have used the LU decomposition method as prescribed in [15] to obtain $\pi_j(x, w)$, the steady-state probability that receiving queue j has w packets at the end of slot x.

---

or two values of i. Thus, this expression can be computed very fast, not in exponential time as implied by the general form presented in the table.

4 Packet-Loss Probability

We now use the queue-length distributions $\pi_{ic}(x, y)$ and $\pi_j(x, w)$ derived in the previous section, to obtain the packet-loss probability at the transmitting and receiving queues.

4.1 The Packet-Loss Probability at a Transmitting Queue

Let Ω_{ic} be the packet-loss probability at the c-th transmitting queue of node i, i.e., the probability that a packet arriving to that queue will be lost. Ω_{ic} can be expressed as:

$$\Omega_{ic} = \frac{E[\# \text{ pkts lost per frame at queue } c, \text{ node } i]}{E[\# \text{ arrivals per frame at queue } c, \text{ node } i]} \quad (11)$$

The expectation in the denominator can be seen to be equal to $M\gamma_{ic}$, where γ_{ic} is the steady-state arrival probability of the arrival process to this queue from (2). To obtain the expectation in the numerator, let us refer to Figure 4(b) which shows the service completion, arrival, and observation instants within slot x. We observe that, due to the fact that at most one packet may arrive in slot x, if the number $v_{ic}(x)$ of slots during which this queue is serviced within arrival slot x is not zero (i.e., $v_{ic}(x) > 0$), no arriving packet will be lost. Even if the c-th queue at node i is full at the beginning of slot x, $v_{ic}(x) \ge 1$ packets will be serviced during this slot, and the order of service completion and arrival instants in Figure 4(b) guarantees that an arriving packet will be accepted. On the other hand, if $v_{ic}(x) = 0$ for slot x, then an arriving packet will be discarded if and only if the queue is full at the beginning of x (equivalently, at the end of the slot before x). Since the 2-MMBP can be in one of two states, we have that the numerator of (11) is equal to $\sum_{x:v_{ic}(x)=0} \sum_{z=0}^{1} \alpha_{ic}^{(z)} \pi_{ic}(B_{ic}, z \mid x \ominus 1)$, where $\ominus$ denotes regular subtraction with the exception that, if $x = 0$, then $x \ominus 1 = M - 1$, and the summation runs over all x for which $v_{ic}(x) = 0$. Using these expressions and the fact that $\pi_{ic}(x) = \frac{1}{M}$ for all x, we obtain an expression for Ω_{ic} as follows:

$$\Omega_{ic} = \frac{\sum_{x:v_{ic}(x)=0} \sum_{z=0}^{1} \alpha_{ic}^{(z)} \pi_{ic}(x \ominus 1, B_{ic}^{(in)}, z)}{\gamma_{ic}} \quad (12)$$

4.2 The Packet-Loss Probability at a Receiving Queue

The packet-loss probability at a receiving queue is more complicated to calculate, since we may have multiple packet arrivals to a given queue within a single arrival slot (refer to Figure 5(a)). Let us define $\Omega_j(n \mid x)$ as the conditional probability that n packets will be lost at receiving queue j given that the current arrival slot is x. A receiving queue will lose n packets in slot x if (a) the queue had $w, 0 \le w \le B_j^{(out)}$, packets at the beginning of slot x, and (b) exactly $B_j^{(out)} - w + n$ packets arrived during slot x. We

126

can then write:

$$\Omega_j(n \mid x) = \sum_{w=0}^{B_j^{(out)}} \pi_j(w \mid x \ominus 1)$$

$$\times Pr[B_j^{(out)} - w + n \text{ pkts arrive to } j \mid x] \quad (13)$$

where $\pi_j(w \mid x \ominus 1) = M\pi(x \ominus 1, w)$ similar to (8). The last probability in (13) can be easily obtained using (9) or (10), as in the last column of Table 2.

Note that at most $u_j(x)$ packets may arrive (and get lost) in arrival slot x. Using (13), we can then compute the expected number of packets lost in slot x as:

$$E[\text{number of packets lost at } j \mid x] = \sum_{n=1}^{u_j(x)} n\Omega_j(n \mid x) \quad (14)$$

The expected number of arrivals to receiving queue j in slot x can be computed as:

$$E[\text{\# arrivals to } j \mid x] = \sum_{s=1}^{u_j(x)} sPr[s \text{ pkts arrive to } j \mid x] \quad (15)$$

Finally, the probability Ω_j that an arriving packet to node j will be lost regardless of the arrival slot x can be found as follows:

$$\Omega_j = \frac{\sum_{x=0}^{M-1} E[\text{number of lost packets at } j \mid x]}{\sum_{x=0}^{M-1} E[\text{number of arrivals to } j \mid x]} \quad (16)$$

5 Numerical Results

We now apply our analysis to a network with $N = 16$ nodes. The arrival process to each of the transmitting queues of the network is described by a different 2-MMBP. The 2-MMBPs selected exhibit a wide range of behavior in terms of two important parameters, the mean interarrival time and the squared coefficient of variation of the interarrival time. The routing probabilities we used are:

$$r_{ij} = \begin{cases} 0.10, & i = 1, \cdots, 16, \ j = 1 \\ 0.06, & i = 1, \cdots, 16, \ j = 2, \cdots, 16 \end{cases} \quad (17)$$

That is, receiver 1 is a hot spot, receiving 10% of the total traffic, while the remaining traffic is evenly distributed to the other 15 nodes. The total rate at which packets are generated by users of the network is 1.98 packets per arrival slot. Most of the traffic is generated at node 1, as the rate of new packets generated at this node is 0.583 packets per arrival slot. The packet generation rate decreases monotonically for nodes 2 to 16. For load balancing purposes, we have allocated one of the C channels exclusively to node 1, since this node receives a considerable fraction of the total traffic. The remaining $C - 1$ channels are shared by the other 15 receivers. The allocation of the receivers to the remaining wavelengths was performed in a round-robin fashion, and is given in Table 3 for $C = 4, 6, 8$.

The quantities a_{ic} of the schedule, i.e., the number of packets to be transmitted by node i onto channel λ_c per frame (refer to Section 2.2 and Figure 2) were fixed to be as close to (but no less than) 0.5 arrival slots as possible. Recall that, while the length of an arrival slot is independent of C and is taken as our unit of time, the length of a service slot

Table 3: Channel sharing for $C = 4, 6, 8$

	$C = 4$	$C = 6$	$C = 8$
$\mathcal{R}_1$	{1}	{1}	{1}
$\mathcal{R}_2$	{2,5,8,11,14}	{2,7,12}	{2,9,16}
$\mathcal{R}_3$	{3,6,9,12,15}	{3,8,13}	{3,10}
$\mathcal{R}_4$	{4,7,10,13,16}	{4,9,14}	{4,11}
$\mathcal{R}_5$		{5,10,15}	{5,12}
$\mathcal{R}_6$		{6,11,16}	{6,13}
$\mathcal{R}_7$			{7,14}
$\mathcal{R}_8$			{8,15}

depends on the number of channels. In cases in which 0.5 arrival slots is not an integral number of service slots, the value a_{ic} is rounded up to the next integer to ensure that every queue is granted at least 0.5 arrival slots of service during each frame [4] (i.e., $a_{ic} = \lceil \frac{N}{2C} \rceil \ \forall \ i, c$). In constructing the schedules, we have assumed that the time it takes a laser to tune from one channel to another is equal to one arrival slot [5]. Finally, for all of the results we present in this section we have let all transmitting and receiving queues have the same buffer capacity B (i.e., $B_{ic}^{(in)} = B_j^{(out)} = B$) to reduce the number of parameters that need to be controlled.

In Figure 6 we show the part of the schedule corresponding to channel λ_1 for three different values of the number of channels $C = 4, 6$, and 8; the parts of the schedules for other channels are very similar. The schedules will help explain the performance results to be presented shortly. Since the number of nodes $N = 16$, for $C = 4$ each arrival slot is exactly four service slots long. Each node is allocated 0.5 arrival slots, or 2 service slots for transmissions on each channel, as Figure 6(a) illustrates. For $C = 4$ the network is *bandwidth limited* [12], that is, the length of the schedule is determined by the bandwidth requirements on each channel ($= 16 \times 0.5 = 8$ arrival slots), not the transmission and tuning requirements of each node ($= 4 \times 0.5 + 4 \times 1 = 6$ arrival slots). The schedule for $C = 6$ in Figure 6(b) is an example where there is a non-integral number of service slots within each arrival slot. More precisely, one arrival slot contains $\frac{N}{C} = \frac{16}{6}$, or $2\frac{2}{3}$ service slots. Each node is assigned two service slots ($a_{ic} = 2$) for transmissions on each channel, since one service slot is less than 0.5 arrival slots. For $C = 6$, the network is again bandwidth limited, and the total schedule length becomes $16 \times 2 = 32$ service slots, or 12 arrival slots.

Finally, when $C = 8$, $a_{ic} = 1$ service slot $= 0.5$ arrival slots, and the corresponding schedule is shown in Figure 6(c). However, in this case the network is *tuning limited* [12], i.e., the node transmission and tuning requirements determine the schedule length. Since each node has to transmit for 0.5 arrival slots on each channel, and to tune to each of the 8 channels (recall that the tuning time is one arrival

---

[4] Other schemes for allocating a_{ic} have been implemented, including setting a_{ic} proportional to r_{ic}, setting a_{ic} proportional to $\max_z \{\alpha_{ic}^{(z)}\}$, and setting a_{ic} to the effective bandwidth [7] of node i's total traffic carried on channel λ_c. Although the packet loss probability results do depend on the actual values of a_{ic}, the overall conclusions drawn regarding our analysis are very similar. Thus, we have decided to include only the simplest case here.

[5] Again, due to the synchronous nature of this network, if one arrival slot is not an integral number of service slots, the number of service slots for which a transmitter cannot transmit is rounded up to the next integer, thereby setting the required time for tuning to some value slightly greater than one arrival slot. As a result, the tuning time is always $\lceil \frac{N}{C} \rceil$ service slots.
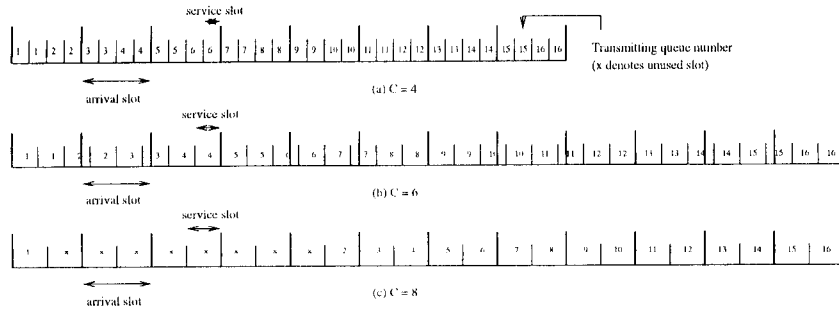
Figure 6: Transmission schedules for λ_1 and $C = 4, 6, 8$

slot), the total schedule length is $8 \times 0.5 + 8 \times 1 = 12$ arrival slots. But the transmissions on each channel only take $16 \times 0.5 = 8$ arrival slots; the remaining 4 arrival slots in Figure 6(c) are not used.

Figures 7-10 show the packet loss probability (PLP) at four different transmitting queues as a function of the buffer size B for $C = 4, 6, 8$. We only show results for two nodes, namely, the node with the highest traffic intensity (node 1) in Figures 7 and 9, and a representative intermediate node (node 8) in Figures 8 and 10. We also consider only transmitting queues 1 and 2 (out of C) at each node. Queue 1 at each node is for traffic to be carried on wavelength λ_1, which is dedicated to receiver 1 (the "hot spot"). Thus, the amount of traffic received by this queue *does not change as we vary the number of channels*, since the first channel is dedicated to receiver 1. Queue 2 at each node is for traffic to be carried on wavelength λ_2. The amount of traffic received by this queue will decrease as the number of channels increases, since channel λ_2 will be shared by fewer receivers. The behavior of queue 2 is representative of the behavior of the other $C - 2$ queues, 3 through C.

Figure 7 plots the PLP $\Omega_{1,1}$ (i.e., the PLP at transmitting queue 1 of node 1) as a function of the buffer size B for $C = 4, 6, 8$. As expected, the PLP decreases as the buffer size increases. For a given buffer size, however, the PLP changes dramatically and counter to intuition, as the number C of channels is varied. Specifically, the PLP increases with C; that is, adding more channels results in worse performance. When B is 10, there is roughly nine orders of magnitude difference between the PLP for $C = 4$ and $C = 8$, and three orders of magnitude difference between $C = 4$ and $C = 6$. As we discussed above, the traffic load of this queue does not change with C; the queue receives the traffic for destination 1, which is always 10% of the total traffic generated at node 1 (see (17)). What does change as C varies is the service rate of the queue, and this change can help explain the results in Figure 7. Referring to Figure 6, we note that when $C = 4$, each frame of the schedule is $M = 8$ arrival slots long, and $a_{1,1} = 2$. Hence, at most 8 packets may arrive to this queue during a frame while as many as 2 packets will be serviced. When $C = 6$, $M = 12$ and $a_{1,1} = 2$, indicating a decrease in the service rate of the queue. Similarly, for $C = 8$, $M = 12$ and $a_{1,1} = 1$, a further decrease in available service per frame for this queue. This decrease is the reason behind the sharp increase in PLP with C in Figure 7. Very similar behavior is observed in Figure 8 where we plot $\Omega_{8,1}$, the PLP at transmitting queue 1 of node 8. The main difference between Figures 7 and 8 is in the absolute values values of PLP. The very small PLP numbers for $\Omega_{8,1}$ are due to the fact that the amount of traffic entering queue 1 of node 8 (0.004 packets per arrival slot) is significantly

smaller than the traffic entering the same queue of node 1 (0.058 packets per arrival slot -- recall that the traffic source were chosen so that the packet generation rate decreases as the node index increases). In fact, for buffer sizes $B = 9$ and $B = 10$ and $C = 4$ our analysis gave PLP values that are essentially zero; these values are not plotted in Figure 8 because we believe that they are the result of round-off errors.

Figures 9 and 10 plot the PLP at transmitting queue 2 of nodes 1 and 8, respectively, against the buffer size. From (17) and Table 3 we note that the traffic received by this queue decreases from 30% of the overall network traffic when $C = 4$ to 18% when $C = 6$ or 8; this decrease is due to the fact that 5 receivers share wavelength λ_2 when $C = 4$, but only 3 receivers share it when $C = 6$ or 8. Thus, the PLP behavior at this queue will depend not only on the change in the service rate as C varies, but also on the change in the amount of traffic received due to addition of new channels. In Figure 9, and for a given buffer size, the PLP decreases as C increases from 4 to 6 (compare to Figure 7). In this case, the decrease in the traffic arrival rate (from an average rate of 0.175 to 0.105 packets per arrival slot) more than offsets the decrease in the service rate that we discussed above. On the other hand, the PLP values for $C = 6$ are less than those for $C = 4$ in Figure 10 (transmitting queue 2 of node 8) due to the fact that the decrease in the offered load (from 0.012 to 0.007 packets per arrival slot) is not substantial enough to offset the decrease in the service rate; still, this increase is less severe than the one in Figure 8 where there was no decrease in the arrival rate. As C increases to 8 there is no change in the offered traffic for either queue; as expected, the PLP rises with the decrease in the service rate.

Finally, Figures 11 and 12 plot the PLP at receiving queues 1 and 8, respectively. Receiving queue 8 is representative of queues 2 through 16 in that it receives 6% of the total network traffic (see (17)). Again, the PLP decreases with increasing buffer size. Also, the lower values of PLP in Figure 12 compared to Figure 11 reflect the fact that only 6% of the total traffic is destined to receiving queue 8, as opposed to 10% for the hot spot queue 1. What is surprising in Figures 11 and 12, however, is that, for a given buffer size, the PLP decreases as the number C of channels increases. This behavior is in sharp contrast to the one we observed in the transmitting side case, and can be explained as follows. First, higher losses at the transmitting queues for larger values of C means that fewer packets will make it to the receiving queues, thus losses will be lower at the latter. But the dominant factor in the PLP behavior in Figures 11 and 12 is the change in the service rate of the receiving queues as C varies (refer to Figure 6). For $C = 4$, as many as 32 packets may arrive to each receiving queue within a

128

frame, and 8 packets may be served (i.e., transmitted to the users). When $C = 6$ the number of potential arrivals in a frame remains at 32, but the frame is 12 arrival slots long, meaning that up to 12 packets may be served, leading to a drop in the PLP. Finally, for $C = 8$ the number of packets served in a frame is the same as in $C = 6$, but the maximum number of packets that may arrive becomes only 16, explaining the dramatic drop in the PLP.

6   Concluding Remarks

In this paper we introduced a model for the media access control (MAC) layer of optical WDM broadcast-and-select LANs. The model consists of a queueing network of transmitting and receiving queues, and a schedule that masks the transceiver tuning latency. We developed a decomposition algorithm to obtain the queue-length distributions at the transmitting and receiving queues of the network. We also obtained analytic expressions for the packet-loss probability at the various queues. Finally, we presented a study case to illustrate the significance of our work in predicting and explaining the performance of the network in terms of the packet-loss probability.

Overall, the results presented in this paper indicate that the performance of a WDM optical network can exhibit behavior that is counter to intuition, and which may not be predictable without an accurate analysis. The performance curves shown also establish that the packet-loss probability in such an environment depends strongly on the interaction among the scheduling and load balancing algorithms, the routing probabilities, and the number of available channels. Our work has made it possible to investigate the behavior of optical networks under more realistic assumptions regarding the traffic sources and the system parameters (e.g., finite buffer capacities) than was possible before, and it represents a first step towards a more thorough understanding of network performance in a WDM environment. Our analysis also suggests that simple slot allocation schemes similar to the ones used for our study case are not successful in utilizing the additional capacity provided by an increase in the number of channels. The specification and evaluation of more efficient slot allocation schemes should be explored in future research.

References

[1] M. Azizoglu, R. A. Barry, and A. Mokhtar. Impact of tuning delay on the performance of bandwidth-limited optical broadcast networks with uniform traffic. *IEEE JSAC*, 14(5):935–944, June 1996.

[2] M. S. Borella and B. Mukherjee. Efficient scheduling of nonuniform packet traffic in a WDM/TDM local lightwave network with arbitrary transceiver tuning latencies. *IEEE JSAC*, 14(5):923–934, June 1996.

[3] Mon-Song Chen, N. R. Dono, and R. Ramaswami. A media-access protocol for packet-switched wavelength division multiaccess metropolitan area networks. *IEEE JSAC*, 8(6):1048–1057, August 1990.

[4] R. Cruz, G. Hill, A. Kellner, R. Ramaswami, G. Sasaki, and Y. Yamabayashi (Eds.). Special issue on optical networks. *IEEE JSAC*, 14(5), June 1996.

[5] J. Jue, M. Borella, and B. Mukherjee. Performance analysis of the Rainbow WDM optical network prototype. *IEEE JSAC*, 14(5):945–951, June 1996.
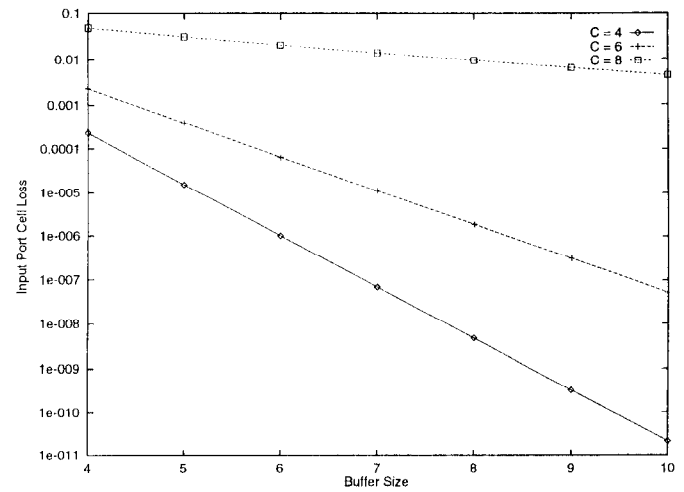
Figure 7: Transmitting queue packet loss probability $\Omega_{1,1}$ for $C = 4, 6, 8$ as a function of buffer size
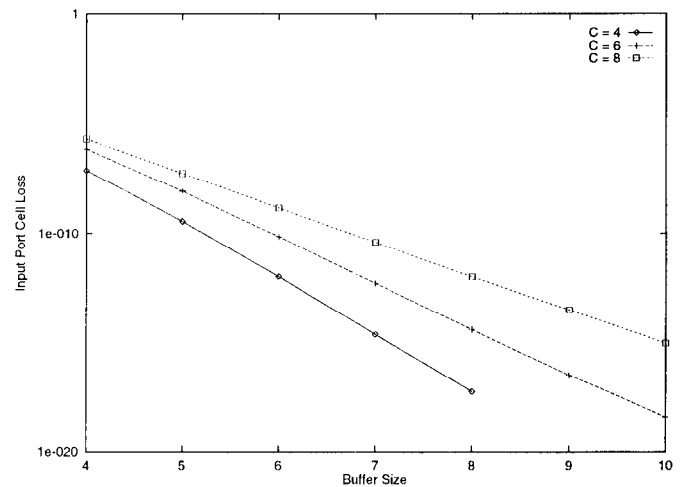

Figure 8: Transmitting queue packet loss probability $\Omega_{8,1}$ for $C = 4, 6, 8$ as a function of buffer size
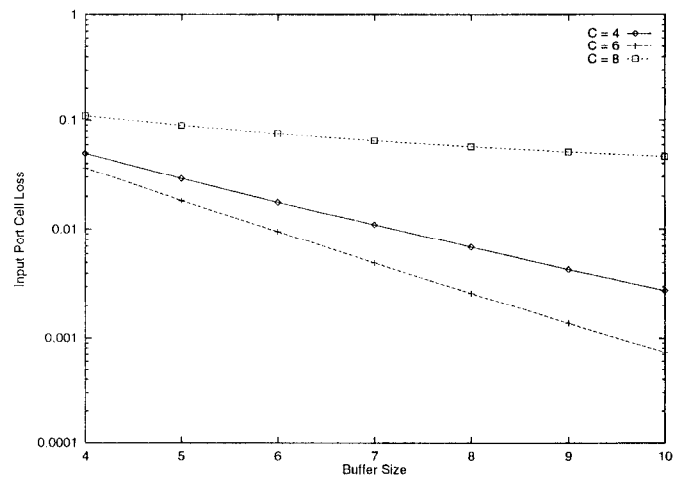

Figure 9: Transmitting queue packet loss probability $\Omega_{1,2}$ for $C = 4, 6, 8$ as a function of buffer size
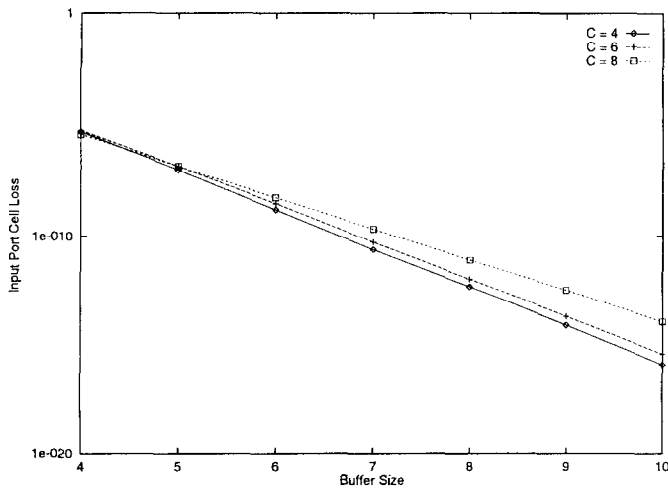
129

Figure 10: Transmitting queue packet loss probability $\Omega_{8,2}$ for $C = 4, 6, 8$ as a function of buffer size
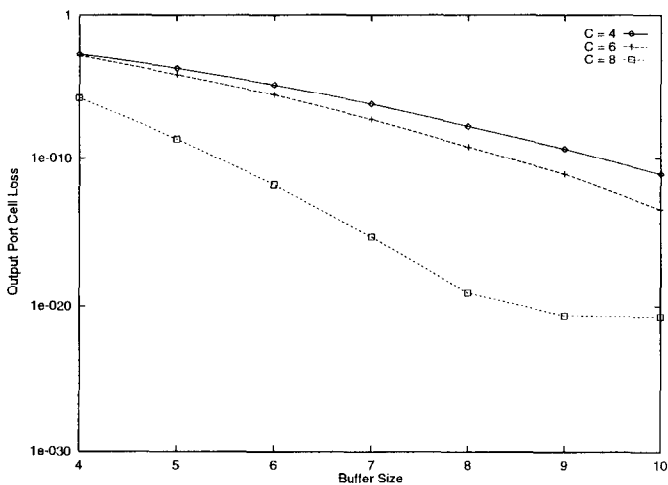

Figure 11: Receiving queue packet loss probability Ω_1 for $C = 4, 6, 8$ as a function of buffer size
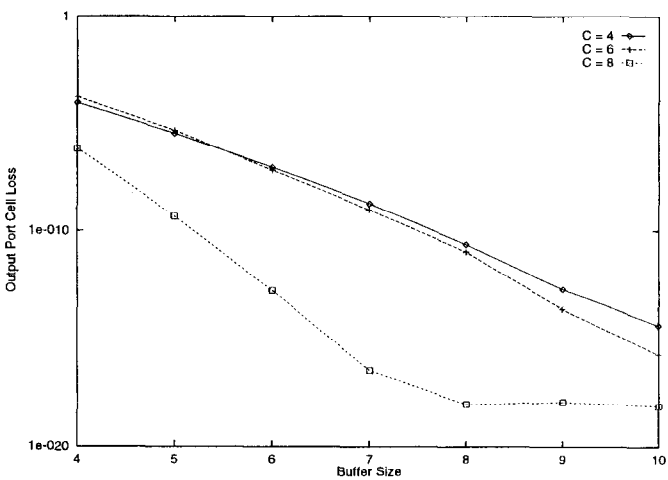

Figure 12: Receiving queue packet loss probability Ω_8 for $C = 4, 6, 8$ as a function of buffer size

[6] Z. Ortiz, G. N. Rouskas, and H. G. Perros. Scheduling of multicast traffic in tunable-receiver WDM networks with non-negligible tuning latencies. In *SIGCOMM '97*, pp. 301–310, Sep. 1997.

[7] H. G. Perros and K. M. Elsayed. Call admission control schemes: A review. *IEEE Communications Magazine*, 34(11):82–91, 1996.

[8] V. Paxson and S. Floyd. Wide area traffic: The failure of poisson modeling. *IEEE/ACM Trans. Networking*, 3(3):226–244, June 1995.

[9] G. Pujolle and H. G. Perros. Queueing systems for modelling ATM networks. In *Int'l Conf. on the Performance of Distributed Systems and Integrated Comm. Networks*, pages 10–12, Kyoto, Japan, September 1991.

[10] D. Park, H. G. Perros, and H. Yamashita. Approximate analysis of discrete-time tandem queueing networks with bursty and correleated input traffic and customer loss. *Operations Research Letters*, 15:95–104, 1994.

[11] G. R. Pieris and G. H. Sasaki. Scheduling transmissions in WDM broadcast-and-select networks. *IEEE/ACM Trans. Networking*, 2(2):105–110, April 1994.

[12] G. N. Rouskas and V. Sivaraman. Packet scheduling in broadcast WDM networks with arbitrary transceiver tuning latencies. *IEEE/ACM Trans. Networking*, 5(3):359–370, June 1997.

[13] V. Sivaraman and G. N. Rouskas. HiPeR-ℓ: A High Performance Reservation protocol with ℓook-ahead for broadcast WDM networks. In *INFOCOM '97*, pages 1272–1279, April 1997.

[14] S. Subramanian, A. K. Somani, M. Azizoglu, and R. A. Barry. A performance model for wavelength conversion with non-poisson traffic. In *INFOCOM '97*, pages 500–507, April 1997.

[15] W. Stewart. *Numerical Solutions of Markov Chains*. Princeton University Press, Princeton, New Jersey, 1994.

[16] S. Tridandapani, J. Meditch, and A. Somani. The MaTPi protocol: Masking tuning times through pipelining in WDM optical networks. In *INFOCOM '94*, pp. 1528–1535, June 1994.

[17] R. W. Wolff. *Stochastic Modeling and the Theory of Queues*. Prentice-Hall, Englewood Cliffs, NJ, 1989.

[18] A. O. Zaghloul and H. G. Perros. Approximate analysis of a discrete-time polling system with bursty arrivals. *Modelling and Performance Evaluation of ATM Technology (Perros, Pujolle, Takahashi Eds.)*, 1993.